Original Research Article

Comparative Characterization of Novel *Schizachyrium Exiles* Leaves and *Raffia Africana Otendor* For Materials Potential

ABSTRACT

The potential for indigenous plant fibers to be used as composites in prospective materials and energy applications is growing all the time. SEM, FTIR, XRD, and XRF were used to investigate the potential of new *Schizachyrium exiles* leaf (SEL) and *Raffia Africana otendor* (RAOL) species. The microporous and macroscopic nature of the materials revealed by SEM analysis can be used as reinforcements in polymers, hybrids, and nano-composite fillers. The presence of the OH group and aliphatic C-O stretching in the FTIR sample revealed a polysaccharide structure. XRD investigations, on the other hand, demonstrate that the crystalline character of RAOL and SEL may be exploited for soft structural designs. Finally, XRF revealed that RAOL and SEL both contain solid minerals (Ca, Si, P, K, Ti, Fe, Mg, Al, and S) that can be extracted and used in a wide range of materials and energy applications, including mesoporous materials, semiconductors, solar and non-solar energy storage devices, rechargeable batteries, and engineering materials.

Keywords: Composite materials, Reinforced fiber, fillers, SEM, XRD, XRF,

1. INTRODUCTION

The use of waste plant resources in composites, hybrids, and fillers is an essential element of applied research (1). When compared to synthetic composites, plant fiber reinforcements offer enhanced material composites in terms of mechanical, thermal, electrical, and rheological properties (2). More study is currently being done on indigenous plant species that have applications in materials and energy consumption. (3).

Several forms of research have established the *Raffia Africana otendor's* feasible potentials, even though several species exist even within the same country. As a result, continuing to characterize and document it aids in a better understanding of it as a material resource. Furthermore, the plant fiber has a wide bandgap and is used in high-temperature, high-power, and high-frequency materials in electrical and solar energy technologies. (4). Another study found that they perform better as epoxy hybrid composites in automotive interior panels. Furthermore, with thermal conductivity of about 0.163 WM-1K-1, the optimal elongation is about 48.9% and can bear a maximum tension of about 340 N/m2 (5). As a

result, it's used to insulate electrical materials, architectural designs, and even kitchen utensils (6,7).

The potential of *Schizachyrium exile* plants as a material resource, on the other hand, has a knowledge vacuum that has to be filled. It thrives in open grassland, peaking in September to November in certain areas and during rainy seasons in others. (8). Lamiaceae refers to a group of nine families of trees and grasses that includes wild plants, herbs, and shrubs. With its remarkable termite resistance capacity, it is locally known as Chen in the Gboko local government region of Benue State, Nigeria, and Himera in Sudan. Chemical farming threatens both species, which are used in craft production, hut thatching, and local bridge construction (9,10). They are utilized locally as feed resources for ruminants in Niger state, Nigeria (11) *Schizachyrium exile* is a reddish-colored annual plant that grows to be around 10-120 cm tall and has few branches on its mild culms. The leaf shape is basal and cauline, and the species is found primarily in tropical Asia, tropical and temperate Africa. (12,13). As a result, *Schizachyrium exile* leaves are researched and compared to *Raffia Africana otendor* for their prospective energy and materials applications for the first time to our knowledge.

2. Material and Methods

2.1. Plant material

The *Raffia Africana otendor leaves* (RAOL) were obtained in the Adar Local Government Area of Ebonyi State, Nigeria, and the *Schizachyrium exile leaves* (SEL) were collected in the Batagarawa Local Government Area of Katsina State. The usual appearance of RAOL and SEL is depicted in the diagram below (figure 1). After collecting the RAOL and SEL leaves, they were extensively washed to eliminate sand and dust particles. Both leaves were sun-dried for 5 days at 27-38 degrees Celsius to achieve brittleness and consistent weight, then ground to a powder and sieved through a 50-mesh sieve. For storage and instrumental analyses, 150 g of each RAOL and SEL powder were measured and stored in a labeled tight plastic container.

Figure 1: *Raffia africana otendor* plant (A) and *Schizachyrium exiles* plant (B).

2.2. Instrumental Analysis

The RAOL and SEL samples were characterized by SEM, XRD, XRF, and FTIR spectroscopy using the previously established standard methods, as briefly detailed below (14–17). The dried samples were inserted in the SEM sample chamber after being mounted on a circular stainless-steel mold and vacuum sputter coated with 10 nm pure gold. The SEM data of the two samples were then obtained using the SEM model created by Phenom world Eindhoven. For FTIR analysis, 2 g of RAOL (sample A) and 200 mg of KBr were ground into a paste in a mortar. Bolt press, cavity rotation, and hydraulic press were used to press the paste together. FTIR spectroscopy was used to examine the sample using Perkin Elmer 8790 series instruments. The scans were carried out at wavelengths ranging from 400 to 4000 cm^{-1}, and the technique was repeated for SEL (sample B). Weighing out 2 g of XRD powder was used to characterize it. The sample was slid into the clips sample holder and the machine door was bolted. The sample was analyzed using the mini-flex software of the (XRD) Equinox 300 model, and the process was repeated for SEL (B). Weighing 1 g of Sample RAOL into XRF slim film was used for the XRF analysis. The film was inserted into the clip cup and carefully secured. Collagen fiber was used to fill the area between the cup and the cap was tightened. The transparent slide was viewed via the cup and analyzed using the software X-supreme 8000 Oxford Instrument USA. For SEL (B), the technique was repeated.

3. Results and Discussion

Figure 2 shows the morphology of Raffia Africana otendor leaves and Schizachyrium exile leaves as studied by SEM. The SEM micrographs of both the RAOL (LHS) and SEL (RHS) samples are shown. Both RAOL AND SEL demonstrated a recurring pattern that remained throughout the whole structure based on the morphological pattern. The SEM inspection of both samples revealed no external characteristics of the particles, such as outlines, flaws, damage, or surface layer. The RAOL SEM picture displays crystallites with tiny grains, but the SEL image shows crystallites with bigger grains. The RAOL looks to be evenly dispersed, however, the SEL pictures appear to be clustered. Furthermore, the micrograph displays RAOL's inherent longitudinal elongation. The in-growth of spherical crystallites covered the full surface of both microscopic and macroscopic holes in both samples. The fibers of the RAOL may be extrapolated from the SEM examination that they are not roundish but longitudinal in shape, indicating that they can be employed for continuous fiber fabrications. In the case of nanocomposite materials and fillers, the surface morphology of these longitudinal fibers/particles is critical. (5,6,16).

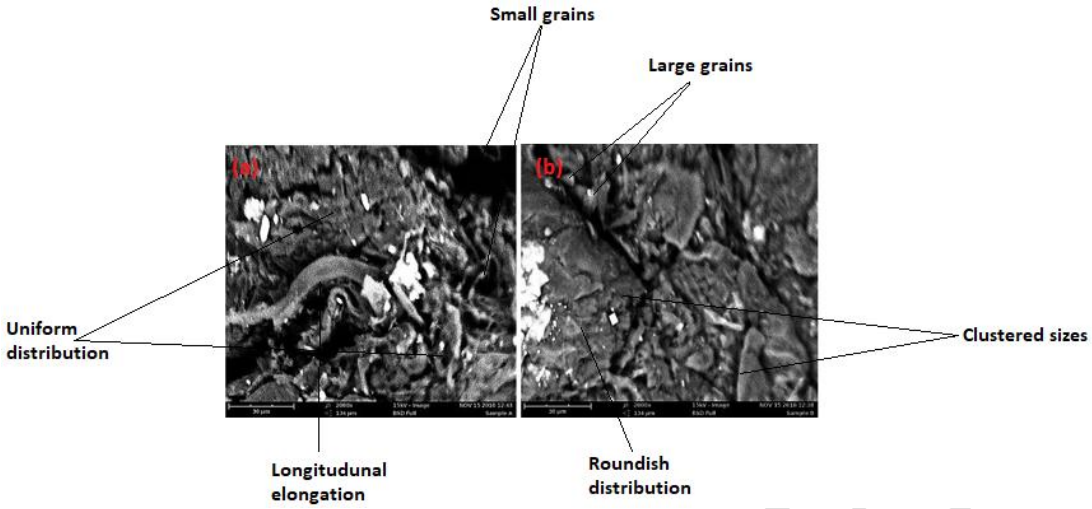

Figure 2: SEM micrograph of (a) *Raffia Africana Otendor* and (b) *Schizachyrium exiles* leaves

The morphological result of SEM in *Schizachyrium exile* leaf indicates roundish rectangular-shaped particle distributions that are apparent throughout the SEM study. It creates a rectangular crystalline distribution with small-scattered grains of equal size. As a result, it has the potential to be utilized as fiber reinforcement in polymer composite materials. As a result, the data strongly suggest that RAOL's longer longitudinal fibers will have a higher density and tensile strength due to the presence of more solid minerals (6,7).

Figures 3 and 4 show the FTIR spectra of RAOL and SEL, respectively. The RAOL and SEL spectra revealed large peaks between 3693 and 3283 cm^{-1} and 3280 cm^{-1}, respectively. The hydroxyl groups (-OH) stretch in RAOL and SEL is allocated to the wide peaks at 3283 and 3280 cm^{-1}. The methyl C-H asymmetry and symmetry bend peaks are located at 2918 cm^{-1} and 2918 cm^{-1}, respectively. The methoxys, methyl ether O-CH_3, and C–H stretch for RAOL and SEL, respectively, are at 2851-2102 cm^{-1} and 2851-2092 cm_{-1}. At 1602 cm^{-1} and 1733 - 1625 cm^{-1}, the conjugated ketone C=C and aryl-substituted C=C stretching of the carboxylic acid of carboxyl groups from hemicelluloses were seen. The conjugated C–O group from aromatic ring stretch in lignin of Raffia Africana otendor and Schizachyrium exile leaves was also suggested by the tiny peak at 1509 cm^{-1} and 1401 cm^{-1}. Furthermore, the C–H group de-formation in cellulose and hemicelluloses is shown by the peak at 1364 - 1319 cm^{-1}. C–O stretch groups from the ether and oxyl compound groups in lignin were ascribed to the 1241 and 1287 cm^{-1} peaks. The C–C vibrations from the saturated aliphatic (alkanes) alkyl group in cellulose have a large peak at 1159 -1028 cm^{-1}. The C=H out-of-plane bound vibration of lignin in RAOL corresponds to the peaks in the 894 cm^{-1} range.

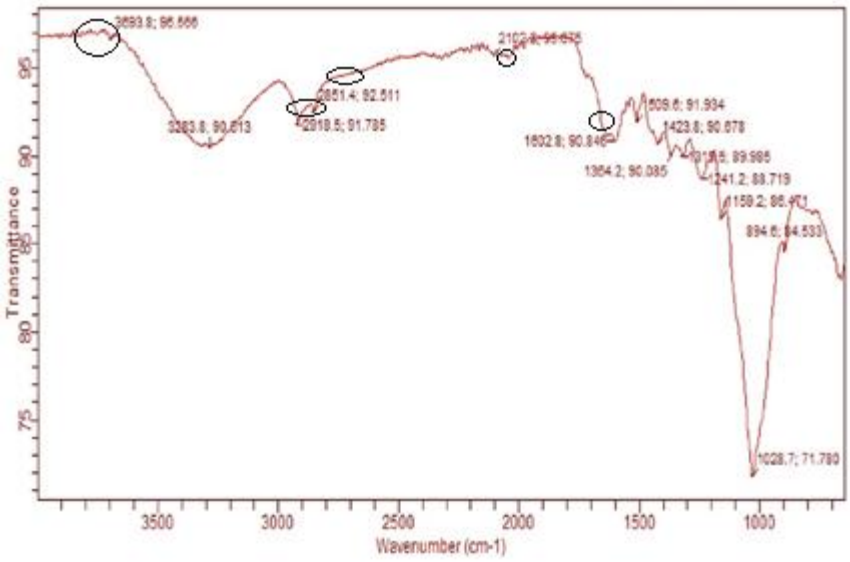

Figure 3: FTIR spectra of *Raffia Africana otendor*

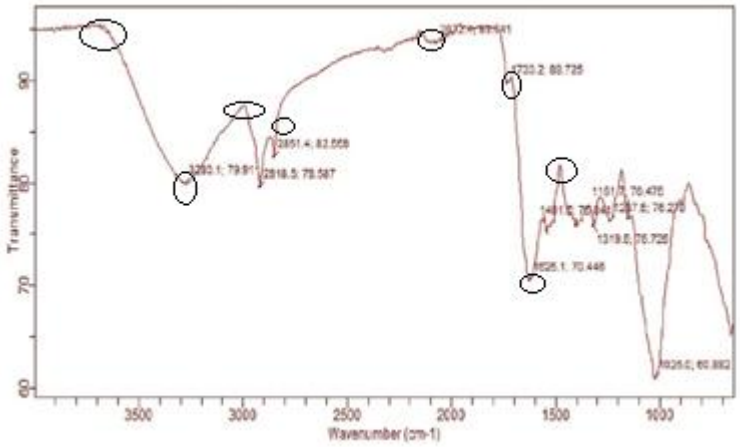

Figure 4. FTIR spectra of *Schizachyrium exile* leaves

Because the side chain of the acetyl group of acetylated xylene was removed during grinding, there was no stretching of the carbonyl group in SEL but it was present in RAOL. The elimination of lignin is further confirmed by the alteration in absorption band in SEL between 1625 and 1025 cm^{-1}. RAOL and SEL spectra also showed variations at peaks between 1602-1159 cm_{-1} and 1625-1287 cm^{-1}, indicating a carboxyl group decrease in both samples. As a result, it was discovered that removing amorphous fiber portions (lignin and hemicellulose) raises the crystallinity index of RAOL and SEL (16). Furthermore, the presence of hydroxyl group (-OH) and aliphatic (C-O) CH stretching implies the presence of polysaccharide structure (15). Peak widening in the (-OH) group may indicate an increase in tensile strength, whereas an increase in the (-OH) group may indicate an increase in tensile strength (18). This conclusion is likewise consistent with the structural explanation provided by the SEM studies. RAOL has a density of 0.7-1.55 g/cm^3 while SEL has a density of 0.5-1.52 g/cm^3. The density of several common synthetic fibers, such as E-glass (2.56 g/cm^3),

carbon fiber (1.4-1.8 g/cm^3), and silica sand (2.4 g/cm^3), was lower. As a result of the functional groups indicated above, both RAOL and SEL may be utilized to make metal roofs and asphalt shingle roofs with reinforcing agents (19). Incorporating RAOL and SEL fibers into composites will also result in the creation of lightweight materials with excellent UV resistance (20,21).

For clarity of significant peaks, the resulting XRD patterns were shown in a 3D graph using Origin 9.0, as shown in figure 5. The RAOL features four notable peaks with strong intensity at theta angles of 10^o, 15^o, 25^o, and 32^o.

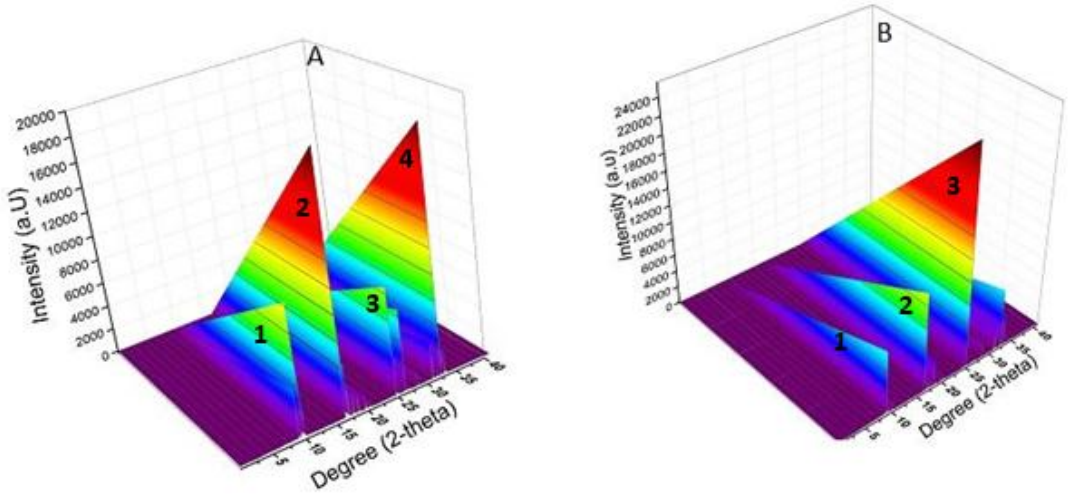

Figure 5. The XRD patterns of RAOL (A) and SEL (B)

Three less noticeable peaks relocated to 10^o, 20^o, and 25^o theta angles on the SEL. Further analysis reveals that the diffraction peaks formed in patterns that corresponded to crystalline phases. The RAOL and SEL have higher diffraction peaks at 700 and 650 cps, respectively, which correspond to SiO_2 and CaO phases. Schizachyrium exiles leave (sample B) had an XRD pattern that was comparable to Raffia Africana Otendor (sample A). SEL, on the other hand, has fewer calcium carbonate phase diffraction peaks than silicones, as revealed in FTIR. The crystallite size and crystallinity index of samples RAOL and SEL influenced the peak broadening.

Due to the extra better diffraction angles, the XRD investigations also demonstrate that there are greater quantities of solid mineral elements/compounds in RAOL than in SEL. Furthermore, the existence of theta at 15/16^o and 25^o confirms the materials' crystalline structure. Due to a rise in tensile strength as seen in FTIR spectrum and SEM investigations, this result provides a hint to possible soft structural design applications (4,18,21).

The weight % of the data obtained from the XRF investigation is shown in figure 6. Both RAOL and SEL have insignificant sodium levels, as seen by the % values displayed. This indicates that Na_2O is not required for the creation and development of SEL and RAOL. Cr_2O_3 and TiO_2 were also at their lowest in SEL, whereas Cr_2O_3 and ZnO were at their lowest in RAOL. Magnesium concentration in RAOL is 1.27, which is seven times lower than SEL's 9.70 wt. percent. This indicates that magnesium plays a critical role in RAOL's cellular

activity. The concentrations of Al_2O_3, Cl, and K_2O in the two samples were not substantially different.

The difference in silicon content between RAOL (Sample A) and SEL (Sample B) was noticeable at 53 Wt % in RAOL (Sample A) and 19.8 Wt % in SEL (Sample B). Furthermore, silicon was found in higher concentrations, suggesting that the material can be used in the production of semiconductors. As a result, rather than absorbing heat, it reflects it to the surroundings. When silicon is extracted, it has the potential to be used in industrial buildings as a composite with clay, silica sand, and stone. It is already used in Portland cement mortar and is suited for both classic and local roofing materials (1,9,22).

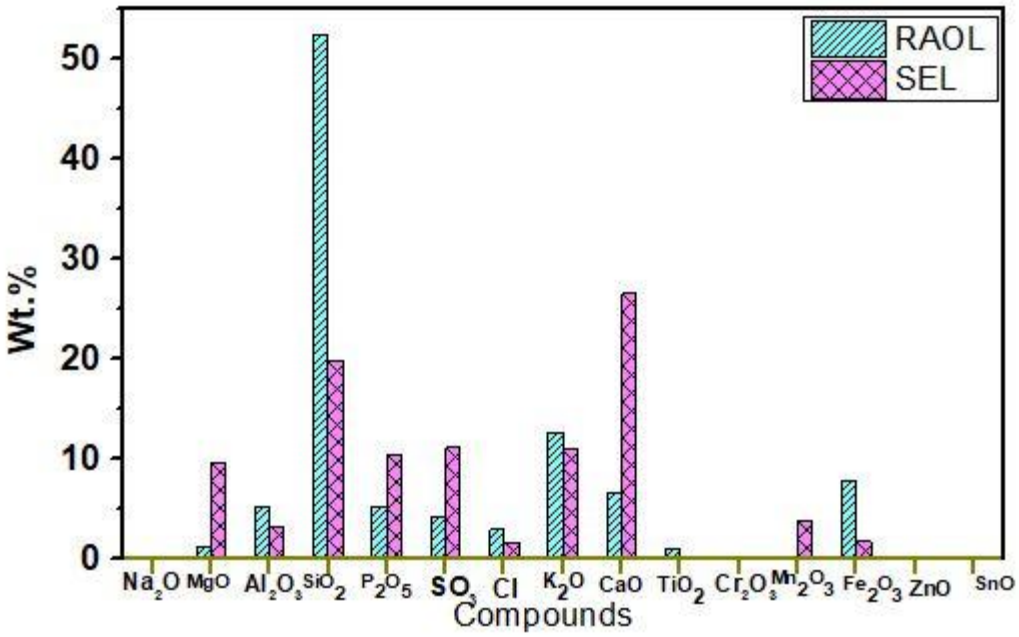

Figure 6. XRF elemental analyses of RAOL and SEL

SEL has double the phosphorus level of RAOL. Phosphorus is a component of nucleic acid and plays a role in energy transfer during photosynthesis. The plant may use more phosphorus to promote frequent blooming and budding, which leads to pollination. As a result, SEL can be used to convert and store energy in phosphorus-based mesoporous materials (23). The sulfur percentage of RAOL and SEL was 4.34 and 11.19, respectively, and they may be used to make lead-acid batteries, glass, and explosives. Furthermore, a new sulfur-based method for storing solar energy has just been developed (24,25). In both samples, the potassium weight percent was greater than 10%. Potassium is an important inorganic cation that controls osmotic potential. As a result, it is required for plant growth. The element can be used to make potassium-ion rechargeable batteries, which might be a cheaper alternative to traditional batteries. (26–28).

Figure 6 depicts the weight percent of data received from the XRF research. The sodium levels in both RAOL and SEL are minimal, as seen by the percent numbers given. This suggests that the presence of Na2O is not essential for the formation and growth of SEL and RAOL. In SEL, Cr2O3 and TiO2 were at their lowest levels, whereas Cr2O3 and ZnO were at their lowest levels in RAOL. RAOL has a magnesium content of 1.27, which is seven times lower than SEL's 9.70 wt%. This suggests that magnesium is important for RAOL's cellular action. The Al2O3, Cl, and K2O concentrations in the two samples were not significantly different. (30).

Both samples have a very low titanium content. It's paramagnetic, having low electrical and thermal conductivity and photocatalytic properties. Because RAOL contains more iron than SEL, RAOL may provide better reinforcement in composite materials and infrastructure construction than SEL (31). Zinc is necessary for the production of chlorophyll. In RAOL and SEL, the amount of tin metal is low and is regarded as a non-essential element. TiO2, ZnO, and ZnO are employed as mesoscopic semiconductors in combination (32). Magnesium hydride-based materials and compounds for hydrogen and energy storage can be made with significant amounts of magnesium (SEL) (33). When used in heat exchange, motor components, vehicle chassis parts, and glazing systems, aluminum can improve energy efficiency, product design, and reduce material waste (34).
On the contrary, when the plant fibers are compared to another natural hemp, kenaf, ramie, sisal fibers, jute, and banana, they all have one thing in common; disposed of as agricultural waste in landfills and incineration. However, through rigorous research, they have found applications as reinforcements and fillers which has triggered the search for further alternatives. It is within this sense that *Raffia Africana Otendor and Schizachyrium exiles* leaves are lagging and needs to quickly find relevance as a conventional fiber-reinforced composite. Such properties expected include high strength, stiffness, low cost, environmentally friendly, and offer improved mechanical and electrical properties (35).

CONCLUSION

SEM, XRD, FTIR, and XRF spectroscopy were used to characterize the leaves of *Raffia Africana Otendor* and *Schizachyrium exiles*. RAOL is found in longitudinal configurations, whereas SEL is found in spherical layouts, according to the findings. Both samples featured the presence of C-H stretching and OH group due to their natural crystallite sizes, which boosts tensile strength and gives them a potential advantage as composites, fillers, and reinforcements. However, inferior mechanical features, increased water absorption, energy absorption, and visco-elastic properties, according to a similar study, continue to limit their efficacy as polymer composites and nanofillers. Regardless, fiber treatment is one of the various options for increasing composite properties. (35). As a result, a full unique mechanical characterization of *Schizachyrium exiles* leaves as a composite material is advised to better understand the mechanical and material behavior. As a result, these plant fibers are expected to eventually replace traditional reinforcements and fillers in material composites. Finally, beyond the SEM, FTIR, XRD, XRF instrumental characterization, expansion, and future studies can be conducted via atomic force microscopy and use of high-resolution transmission electron microscope to understudy the surface roughness and morphological orientation.

References

1. Saba N, Tahir M, Jawaid M. Review on the potentiality of nano filler/natural fiber filled polymer hybrid composites. Polymer (Guildf). 2014;6:2247–73.
2. Mahmud S, Hasan KMF, Jahid MA, Mohiuddin K, Zhang R, Zhu J. Comprehensive review on plant fiber-reinforced polymeric biocomposites. J Mater Sci. 2021;56(12):7231–64. Available from: https://doi.org/10.1007/s10853-021-05774-9
3. Dixit S, Goel R, Dubey A, Shivhare PR, Bhalavi T. Natural Fibre Reinforced Polymer Composite Materials - A Review. Polym from Renew Resour. 2017;1;8(2):71–8. Available from: https://doi.org/10.1177/204124791700800203
4. Ufere E, Okpala O. Synthesis and Characterization of undoped raffia palm and oil

bean doped lead chloride (PbCl2) crystal in silica Gel. Int J Sci Eng Res. 2016;7(1):583–92.
5. Nyior G., Aye S., Tile S. Study of Mechanical Properties of Raffia Palm Fibre/Groundnut Shell Reinforced Epoxy Hybrid Composites. J Miner Mater Charact Eng. 2018;6:179–92.
6. James R, Tamunoiyowuna S. Investigation of Thermal Conductivity of Raphia Fibre (Piassava) from Raphia Hookeri. Int J Appl Sci Math Theory. 2016;2(2):11–7.
7. Odera R, Onukwuli O, Osoka E. Stress and Strain Characteristics of Raffia Palm Fibre under Varying Conditions. Int J Chem Eng Res. 2011;3(2):159–66.
8. Mitra S, Soban K. Biodiversity impact and assessment: Diversity of grass flora of West Bengal with special reference to their utility. 2nd ed. Jaipur: India: Pointer Publishers.; 2011. 23–109 p.
9. Shomkegh S, Mbakwe F, Sale F. Ethno botanical Survey of Wild Plants Utilized for Craft Making and Local Construction among the Tiv People of Benue State, Nigeria. J Agric Ecol Res Int. 2016;9(3):1–11.
10. Sulieman HM, Buchroithner MF, Elhag MM. Use of local knowledge for assessing vegetation changes in the Southern Gadarif Region, Sudan. Afr J Ecol. 2012 1;50(2):233–42. Available from: https://doi.org/10.1111/j.1365-2028.2011.01318.x
11. Nourou A, Nasreldin B, Abdoulaye S, Ignatius V. Effect of urea treatment of roughages and in vitro ingestibility of available feed resources in Maradi area of Niger. Am J Agric For. 2018;6(4):78–83.
12. Ibrahim Author. K (Kamal M. Grasses of Mali. Washington, D.C. : Smithsonian Institution Scholarly Press,
13. Arthan W, McKain MR, Traiperm P, Welker CAD, Teisher JK, Kellogg EA. Phylogenomics of Andropogoneae (Panicoideae: Poaceae) of Mainland Southeast Asia. Syst Bot. 2017:1;42(3):418–31. Available from: https://doi.org/10.1600/036364417X696023
14. Elenga R., Djemia P, Tingaud D, Chauveau T, Maniongui J., Dirras G. Effects of alkali treatment on the microstructure, composition, and properties of the Raffia textile fiber. Bioresources. 2013;8(2):2934–49.
15. Majekodunmi U. Characterization of Raphia Hookeri gum for the purpose of being used as a pharmaceutical excipient. World J Pharm Res. 2016;5(2):86–97.
16. Odera R, Onukwuli O, Atunanya C. Characterization of the thermo-microstructural analysis of raffia palm fibers proposed for roofing sheet production. J Miner Matererials Charact Eng. 2015;3:335–43.
17. Ahmed A, Abdullah M, Wood K, Hamza M, Othman R. Determination of some trace elements in marine sediment using ICP-MS and XRF (A Comparative Study). Orient J Chem. 2016;29(3):645–53.
18. Fadele O, Oguocha INA, Odeshi A, Soleimani M, Karunakaran C. Characterization of raffia palm fiber for use in polymer composites. J Wood Sci. 2018;64(5):650–63. Available from: https://doi.org/10.1007/s10086-018-1748-2
19. Foster B. Establishment, Competition and the Distribution of Native Grasses among Michigan Old-Fields. J Ecol. 1999;87(3):467–89.
20. Danewalia SS, Sharma G, Thakur S, Singh K. Agricultural wastes as a resource of raw materials for developing low-dielectric glass-ceramics. Sci Rep. 2016;6(1):24617. Available from: https://doi.org/10.1038/srep24617
21. Eze-Uzomaka O, O. Nwadiuto O. Appraisal of coir fiber- cement mortar composite for low-cost roofing purposes. African J Sci Technol. 2009;8(1):6–15.
22. Mohammed L, Ansari M, Pua G, Jawaid M, Islam S. A review on natural fiber reinforced polymer composite and its applications. Int J Polym Science. 2015; Article ID:1–15.
23. Mei P, Kim J, Kumar NA, Pramanik M, Kobayashi N, Sugahara Y, et al. Phosphorus-Based Mesoporous Materials for Energy Storage and Conversion. Joule.

2018;2(11):2289–306. Available from: https://www.sciencedirect.com/science/article/pii/S2542435118303477
24. Seyfaee A, Jafarian M, Moumin G, Thomey D, Corgnale C, Sattler C, et al. Integration assessment of the hybrid sulphur cycle with a copper production plant. Energy Convers Manag. 2021;249:114832. Available from: https://www.sciencedirect.com/science/article/pii/S0196890421010086
25. Liu C, He Z, Li Y, Liu A, Cai R, Gao L, et al. Sulfur contributes to stable and efficient carbon-based perovskite solar cells. J Colloid Interface Sci. 2022;605:54–9. Available from: https://www.sciencedirect.com/science/article/pii/S0021979721011255
26. Hwang J-Y, Myung S-T, Sun Y-K. Recent Progress in Rechargeable Potassium Batteries. Adv Funct Mater. 2018 Oct 1;28(43):1802938. Available from: https://doi.org/10.1002/adfm.201802938
27. Xu Y-S, Duan S-Y, Sun Y-G, Bin D-S, Tao X-S, Zhang D, et al. Recent developments in electrode materials for potassium-ion batteries. J Mater Chem A. 2019;7(9):4334–52. Available from: http://dx.doi.org/10.1039/C8TA10953B
28. Wang H, Wang Y, Wu Q, Zhu G. Recent developments in electrode materials for dual-ion batteries: Potential alternatives to conventional batteries. Mater Today. 2021; Available from: https://www.sciencedirect.com/science/article/pii/S1369702121003953
29. Yuan Y, Li Y, Zhao J. Development on Thermochemical Energy Storage Based on CaO-Based Materials: A Review. Vol. 10, Sustainability. 2018.
30. Chen W, Li G, Pei A, Li Y, Liao L, Wang H, et al. A manganese–hydrogen battery with potential for grid-scale energy storage. Nat Energy. 2018;3(5):428–35. Available from: https://doi.org/10.1038/s41560-018-0147-7
31. Razzaq A, Ajaz T, Li JC, Irfan M, Suksatan W. Investigating the asymmetric linkages between infrastructure development, green innovation, and consumption-based material footprint: Novel empirical estimations from highly resource-consuming economies. Resour Policy. 2021;74:102302. Available from: https://www.sciencedirect.com/science/article/pii/S0301420721003123
32. Hoye RLZ, Musselman KP, MacManus-Driscoll JL. Research Update: Doping ZnO and TiO2 for solar cells. APL Mater. 2013; 1;1(6):60701. Available from: https://doi.org/10.1063/1.4833475
33. Yartys VA, Lototskyy M V, Akiba E, Albert R, Antonov VE, Ares JR, et al. Magnesium based materials for hydrogen-based energy storage: Past, present, and future. Int J Hydrogen Energy. 2019;44(15):7809–59. Available from: https://www.sciencedirect.com/science/article/pii/S0360319919300072
34. Haraldsson J, Johansson MT. Energy Efficiency in the Supply Chains of the Aluminium Industry: The Cases of Five Products Made in Sweden. Vol. 12, Energies. 2019.
35. Fadele O, Oguocha INA, Odeshi AG, Soleimani M, Tabil LG. Effect of chemical treatments on properties of raffia palm (Raphia farinifera) fibers. Cellulose. 2019;26(18):9463–82. Available from: https://doi.org/10.1007/s10570-019-02764-8
36 Ramesh M. Hemp, jute, banana, kenaf, ramie, sisal fibers. Handbook of Properties of Textile and Technical Fibres, 2018; 301–325. doi:10.1016/b978-0-08-101272-7.00009-2